Erasure Mechanisms of Polarization Holographic Gratings in Spirooxazine-Doped Polymer Films

Shencheng Fu,[1] Weilin Hu,[2] Minggui Xie,[2] Yichun Liu,[3] Qingduo Duanmu[1]

[1]*School of Science, Changchun University of Science and Technology, Changchun, 130022, People's Republic of China*
[2]*Faculty of Chemistry, Sichuan University, Chengdu, 610064, People's Republic of China*
[3]*Center for Advanced Optoelectronic Functional Material Research, Northeast Normal University, Changchun 130024, People's Republic of China*

ABSTRACT: Dynamic holographic recording under linear polarized writing beams at 632.8 nm was performed on two different new spirooxazine doped PMMA matrices assisted by UV light. Thermal rate constants of the two holographic storage medium were determined. It was found that diffraction efficiency and erasure dynamics of the holographic gratings in the two polymer films were dependent on the thermal stability and aggregation of spirooxazine molecules in PMMA matrices. During erasure of the holographic gratings, only in the polymer film with a lower thermal rate constant, a nearly instantaneous increase of diffraction efficiency was observed, resulting from the formation of a transient orientation grating. A theoretical description of the transient orientation grating, competing with isomerization gratings, agrees well with experimental results. The interaction between the chromophores and matrices was also discussed. © 2008 Wiley Periodicals, Inc. J Appl Polym Sci 111: 2157–2162, 2009

Key words: orientation; isomerization; matrix; erasure; films

INTRODUCTION

Spirooxazines (SOs) are reversible photochromic compounds. At room temperature, in the dark, they exist as an uncoloured closed structure; upon ultraviolet irradiation the C_{spiro}—O bond is broken and then isomerized into colored open forms which are called *trans*-merocyanines (*trans*-MCs). *trans*-MCs can revert to the initial spiro forms thermally or photochemically.[1,2] The ultrafast electro-cyclization reaction is supposed to involve an intermediate also having zwitterionic character. This molecular state is called *cis*-merocyanines (*cis*-MCs). The lifetime of *cis*-MC is relatively shorter than that of *trans*-MC due to its higher energy (Fig. 1).[3] However, *cis*-MC could be trapped by metal ion. The evidence of the *cis*-MC isomer form was observable by UV-Vis spectrophotometry over a significant time period.[4] The reversible conversion between SO and MC has been extensively investigated due to their potential applications in lenses of variable optical density, displays, filters, and optical-memory devices.[5,6,7] For example, spriooxazine doped polymer films could be candidates for holographic storage medium. Recently, polarization holographic recording in spriooxazine doped polymer films was realized in visible wave band after UV preirradiation.[8–10] However, little is known about the erasure mechanism of the polarization holographic grating in spriooxazine doped polymer films. In this work, thermal rate constants of two different new spirooxazine doped polymer films were compared. Competition among SO, *cis*-MC and *trans*-MC was described. It was demonstrated that the erasure of holographic gratings in spirooxazine doped polymer films involved the formation of transient orientation gratings, resulting from the orientation of *trans*-Merocyanine. The theoretical description of the transient orientation grating, competing with isomerization gratings, agrees well with experimental results. These results may be helpful to the application of erasable holographic recording.

EXPERIMENTAL

Recording material

6'-Piperidino-1,3,3-trimethylspiro[indolino-2,3'-[3H]naph- tha- [2,1-b][1,4]oxazine (SO$_1$) and 6-cyano-1,3,3-trimethylspiro[indolino-2,3-[3H]naphtha-[2,1-b][1,4]oxazine] (SO$_2$) were synthesized with microwave irradiation. The synthetic routes for SO$_1$and SO$_2$ are shown in Scheme 1. The structure of SO$_1$ was tested

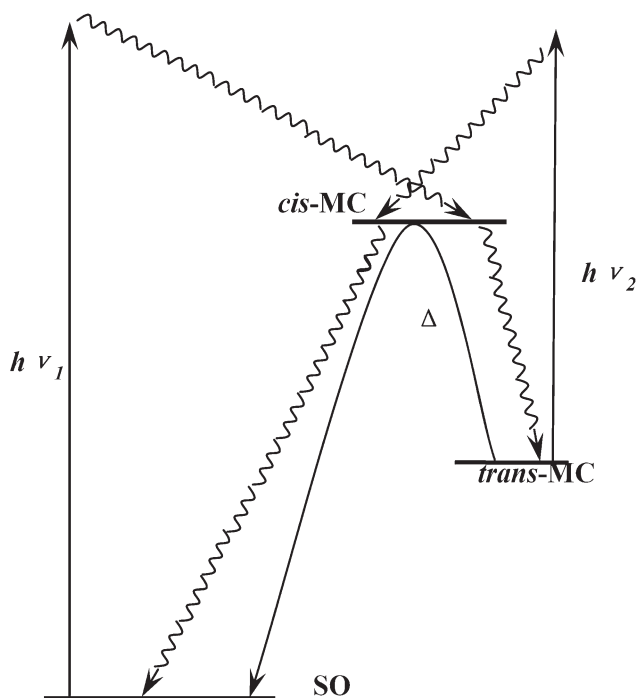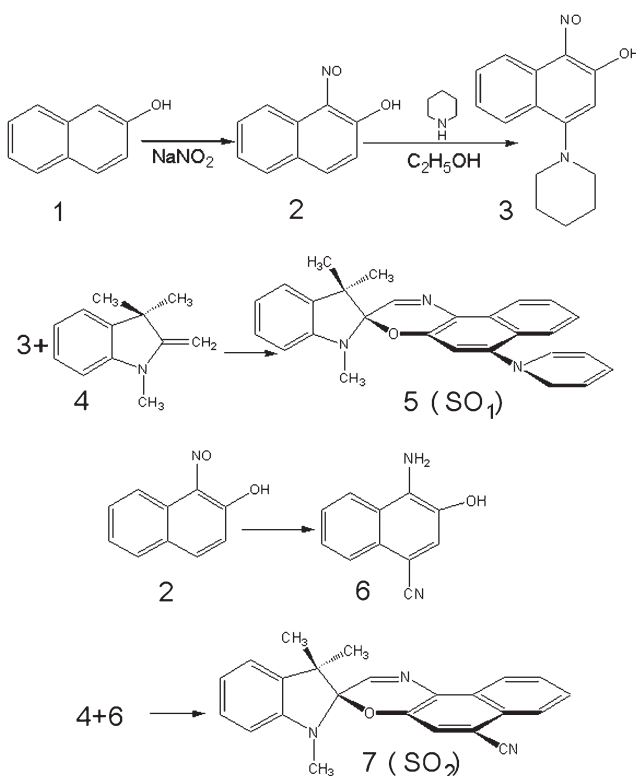**Figure 1** Qualitative energy profile for the photochromic reaction of spirooxazines.

by FTIR and ^{1}H-NMR. From the FTIR spectrum, a few bands can be identified: 2963 cm^{-1} (s, =C—H), 1613 cm^{-1} (m, C=N), 1183 cm^{-1} (m, C—O—C). ^{1}H-NMR measurements were also carried out using a

Scheme 1 Synthetic route for the target compound.

Bruker DMX-400 instrument operating at 400 MHz. ^{1}H-NMR spectrum also indicated (CD$_3$SOCD$_3$, δ, ppm): 1.35(6H, 2 × CH$_3$), 1.84(6H, 3 × CH$_2$), 2.75 (3H, N—CH$_3$), 3.04(4H, 2 × N—CH$_2$) 8.5–8.7(10H, Ar—H). The structure of SO$_2$ was confirmed by melting point and elementary analysis: 431.9–432.8 K; analysis calculated for C$_{23}$H$_{19}$N$_3$O: C 78.07(78.63), H 5.33(5.41), N 11.74(11.96); MS *m/z*(M) 353(100%), 338(45%), 159(90%), 144(27%).

Recording film preparation and holographic recording

Commercially available poly(methyl methacrylate) (PMMA) was used without further purification. Recording medium for holographic optical recording was prepared by solubilizing 5 mg SO$_{1(2)}$ and 100 mg PMMA in chloroform (20 mL), then spin-coating the homogeneous solution on a glass substrate (18 × 18 × 0.17 mm^3) with a spin rotation speed of 1500 rpm. The thickness of the film was about 10 μm measured with a Precision Ellipsometer. The film was dried in air and kept in darkness at room temperature. It was found that PMMA has a better film quality than some other matrices, such as PVC and EPDM.

Holographic recording measurements were made possible by two interferential laser beams irradiating the sample, as shown in Figure 2. The major elements of the experimental setup were a linearly polarized He-Ne laser (632.8 nm) which generated the writing and reading beams. The diameter of the laser beams was ∼ 0.3 cm, and the intersecting angle between the beams was ∼ 10°. A mercury-arc lamp (125 mW) was used to irradiate the sample with homogenous, incoherent light at 365 nm. And the power density of the mercury arc lamp at the sample location was about 1 mW/cm^2. The diffractive signals were registered on a photodiode interfaced with a computer.

RESULTS AND DISCUSSION

Photochromism of spirooxazine-doped polymer films

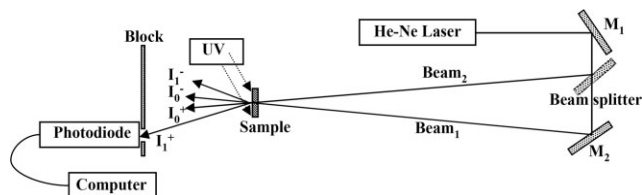The UV–Vis spectra were measured using a Perkin–Elmer Lambda 900 spectrophotometer. Figure 3(a)

Figure 2 Experimental configuration for the recording of holographic gratings by He-Ne laser beam$_1$ and beam$_2$. *M* denotes mirror.
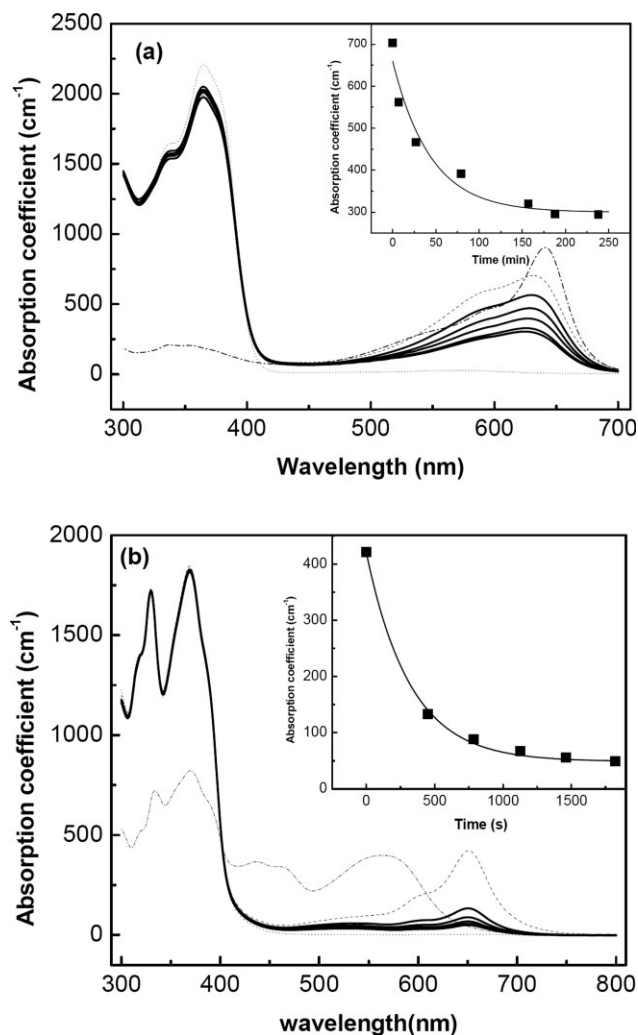
Figure 3 UV-Vis spectrum of PMMA film doped with 5 wt % (a) SO_1 and (b) SO_2 (dotted lines), the corresponding spectrum after UV-induced isomerization of SOto MC (dashed lines) and changes in the absorbance spectra of MC in darkness (solid lines). The dash dot lines are the spectrum of SO doped in CHCl₃ after UV irradiation with the concentration of 0.01 mg/mL. The inset is the absorption coefficient at 633 nm according to the time the UV light is switched off. The square dots are the experimental measurements. The solid line is the theoretical fit.

shows typical UV–Vis spectra of PMMA film containing SO_1 and the corresponding UV-induced MC_1, as dotted lines and dashed lines, respectively. Figure 3(b) shows the similar spectra for SO_2-MC_2 systems in PMMA film. Thermal relaxations of MC_1 and MC_2 in darkness (25°C) are also shown in Figure 3(a,b), respectively (solid lines). The insets of Figure 3(a,b) are the absorption coefficient of MC_1 and MC_2 at 633 nm as a function of the time the UV light is switched off, respectively. For comparison, the UV–Vis spectra of MC_1 and MC_2 in dilute chloroform solution are also shown in Figure 3(a,b), respectively (dash dot lines). A detectable spectral

red-shift of the SO_2 doped in polymer matrices relative to that in dilute solution was observed in Figure 3(b), indicating a very strong J-aggregation of $trans$-MC_2 molecules in the polymer films.[11] The decoloration dynamic at 633 nm was fitted by the following equation:

$$\ln\left(\frac{A_t - A_\infty}{A_0 - A_\infty}\right) = -ki \cdot t, \qquad (1)$$

where A_t, A_0 and A_∞ are the absorbencies at $\lambda = 633$ nm at times t, zero and infinity, respectively. Thermal rate constants, $k_1 = 3.7 \times 10^{-4}$ (s^{-1}) and $k_2 = 3.1 \times 10^{-3}$ (s^{-1}), are obtained, for SO_1-MC_1 and SO_2-MC_2 systems in PMMA films, respectively. After about 4 h the SO_1 doped polymer film still contains many MC_1 molecules. In the dark, with UV irradiation, $trans$-MC_1 is dominant in SO_1-MC_1 systems. However, $trans$-MC_2 is more unstable than $trans$-MC_1, which reduced the quantum yield from SO_2 to $trans$-MC_2 under UV irradiation. With UV irradiation, SO_2-MC_2 systems in the dark involve a mixture of all the species associated with the Scheme 2.

Holographic recording and erasure

Figure 4 shows the first-order diffractive signal of the holographic gratings in the SO_1 doped polymer film generated by two He-Ne laser beams with the same (s, s) polarization. The power density of each beam was 10/0.07 mW/cm². The experimental sequences are described as follows: with the UV source on, the two linearly polarized He-Ne beams irradiated the sample and the intensity of the measured diffractive signal increased gradually to a fix value (marked as point A). When one He-Ne beam was switched off with the UV source on, the diffractive-signal intensity increased sharply to a maximal value (marked as point B) and then decreased slowly approaching a constant value at point C. A similar temporal evolution was observed in the repeated process.

Our explanation is the following. $trans$-MC has an extremely large dipole moment because of its ionic form.[12] Hence, linearly polarized pumping beams will induce the rapid reorientation of $trans$-MC. While the dipole moments of SO and cis-MC is relatively small for the short distance between the positive and negative charge sites. The stereo structure of cis-MC also produced a strong steric hindrance in the PMMA matrix. Therefore, the orientations of SO

$$SO \rightleftharpoons cis\text{-}MC \rightleftharpoons trans\text{-}MC$$
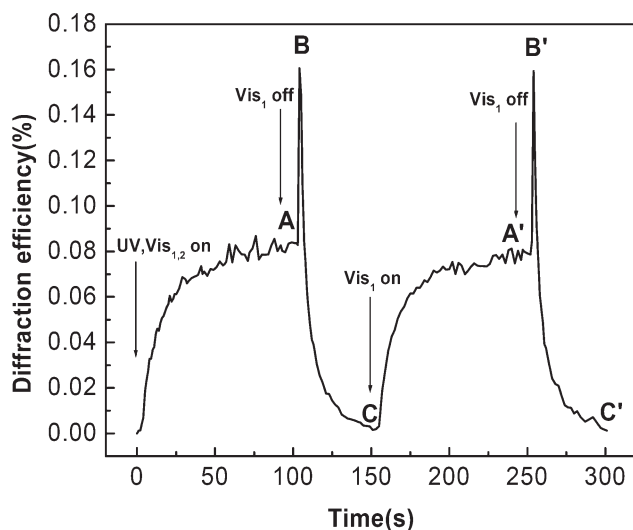
Scheme 2 Reaction route for SO-MC system.

Figure 4 The first-order diffractive signal of the holographic gratings assisted by UV-light versus time in SO_1 doped PMMA films. "On" means UV-light or visible lights (He-Ne laser beam$_1$ or beam$_2$) are turned on and "off" means UV-light or visible light (He-Ne laser beam$_1$) is turned off.

and *cis*-MC irradiated by the linearly polarized pumping beams is neglected.

The more stable colored *trans*-MC$_1$ isomers with random orientation were expected to be the dominant form with solely UV irradiation in the dark regions of the interference pattern. While in the bright regions of the interference pattern, with both the UV and He-Ne beam irradiating the sample, chemical species equilibrium between SO$_1$ and MC$_1$ and reorientation equilibrium for MC$_1$ molecules are reached.[13] As the power density of He-Ne laser is much higher than that of UV lamp, *trans*-MC$_1$ is the minority form in the bright regions. So the isomerization grating, formed by periodic distributions of SO$_1$ and MC$_1$, is dominant at point A. When one He-Ne beam is switched off with the UV source on, the spatial modulation of the He-Ne beams disappeared. *trans*-MC$_1$ molecules in the initial dark regions was rapidly orientated by the polarized He-Ne beam. A transient orientation grating is formed at point B, resulting in the rapid increase of the diffractive-signal. At the same time, the He-Ne laser also drives conversion of *trans*-MC$_1$ to SO$_1$. Finally, the same chemical species equilibrium and reorientation equilibrium in the initial dark regions, as that in the initial bright regions, were reached. So the intensity of the diffracted signals almost drops to zero at point C. Figure 5 shows the molecular distributions in the SO$_1$ doped polymer film at point A, B, and C.

For the low power density are introduced in the photochromic system, a pseudofirst-order process without nonlinear effects describing the present sys-

tem are reasonable. The diffraction efficiency versus time from point A to C can be simply expressed as

$$\eta(t) = \eta_{\text{isomer}} \exp[-R_B \cdot (t - t_A)] + \eta_{\text{orient}} \exp[-R_B \times (t - t_A)]\{1 - \exp[-O_B \cdot (t - t_A)]\} \quad (1)$$

$$t \geq t_A (= 100s) \quad (2)$$

where η_{isomer} and η_{orient} are the maximum of diffraction efficiency for isomerization gratings and orientation gratings, respectively. R_B and O_B are the rate constants for forming isomerization and orientation gratings by He-Ne lasers, respectively. The theoretical description [eq. (1)] of the competition between orientation gratings and isomerization gratings, agrees well with experimental results, as shown in Figure 6. $R_B = 0.17s^{-1}$ and $O_B = 4.53s^{-1}$ were obtained.

To exclude the effect of UV light on the formation of the transient orientation grating, the SO$_1$ doped polymer film was initially exposed to the UV excitation beam, until maximal coloring occurred, then separately exposed to two parallel polarized He-Ne beams (632.8 nm) of 10 mW. On turning on the He-Ne laser, the diffractive signal rapidly reaches a maximum value, and then drops slowly. At 63s, one He-Ne beam was switched off, a slight increase was observed (Fig. 7). It was indicated that without UV companion, quite a number of *trans*-MC$_1$ molecules still formed the transient orientation grating.

The temporal evolution of diffraction efficiency for the SO$_2$ doped polymer film was shown in Figure 8.
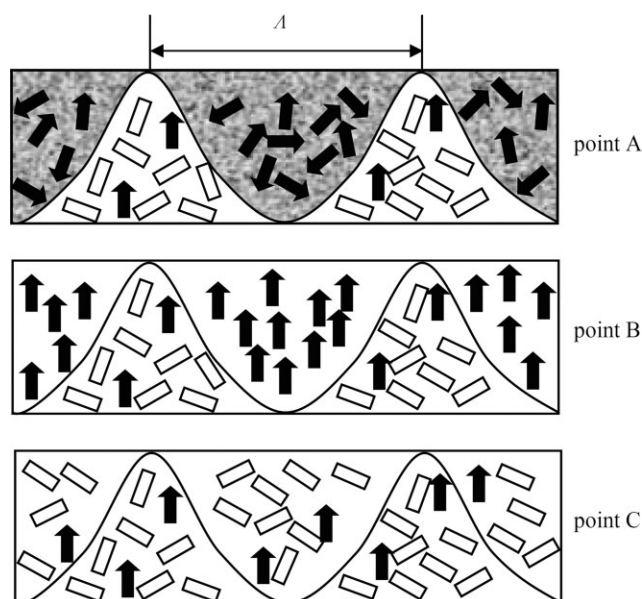

Figure 5 The sketch map of the transformation of SO$_1$-MC$_1$ system from point A to C in Figure 4. Λ is grating period.
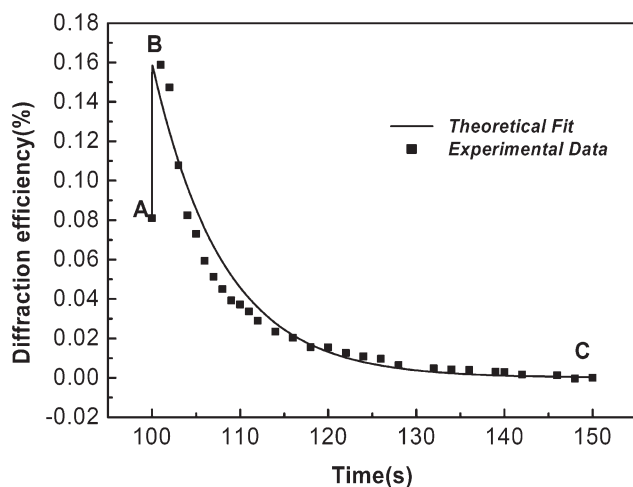
Figure 6 The theoretical fit of the competition between orientation gratings and isomerization gratings (solid line) to the experimental results from point A to C in Figure 4 (dots).

Figure 8 The first-order diffractive signals of the holographic gratings recorded by two He-Ne beams versus time accompanied with UV irradiation in SO_2 doped PMMA films.

Differently, when one He-Ne beam was switched off with the UV source on, the diffractive-signal only decreased approaching a constant without any observable peak. Furthermore, diffraction efficiency of the SO_2/PMMA film is much lower than that of the SO_1/PMMA film. Even with UV irradiation, significant populations of SO_2 and cis-MC$_2$ existed in the dark regions of interference fringe due to the instability of $trans$-MC$_2$. During recording of holographic gratings, thermal effect of He-Ne beams on the polymer further decrease the proportion of the $trans$-MC$_2$ isomers to the other two species. When one He-Ne beam is switched off, the limited popula-

tion of $trans$-MC$_2$ could not induce the apparent orientation gratings. So the diffractive signal drops directly. Additionally, the J-aggregate formation in the SO_2 doped polymer film restrained the orientation of $trans$-MC$_2$ to a certain extent. Conversely, for the aggregation of $trans$-MC$_1$ in PMMA matrices is so weak [Fig. 3(a)], the formation of the transient orientation grating in the SO_1 doped polymer film is relatively easy to be observed.

CONCLUSIONS

The erasure mechanism of polarization holographic gratings in two different spirooxazine doped polymer films was investigated in detail. Diffraction efficiency and erasure dynamics of the polarization holographic gratings in the two polymer films were dependent on the thermal stability and aggregate of spirooxazine molecules in PMMA matrices. The theoretical description of the transient orientation grating, competing with isomerization gratings, agrees well with experimental results. These results may be of great help to the application of spirooxazine doped polymer films in erasable holographic storage.
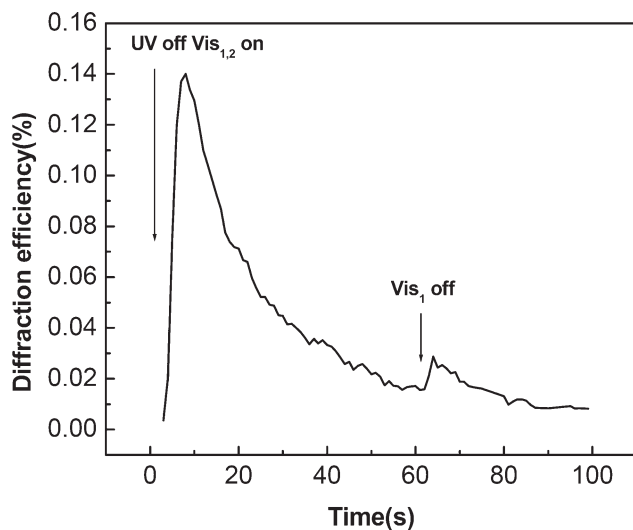

Figure 7 The first-order diffractive signal of the holographic gratings preirradiated by UV-light versus time with the same polarized recording beams. At 63s, He-Ne beam 1 was switched off.
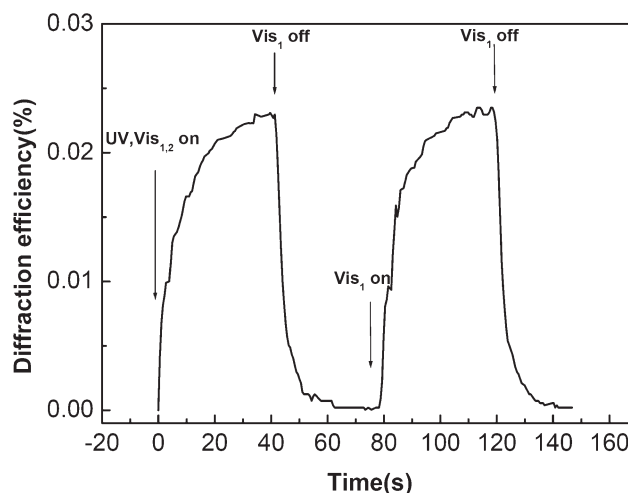
References

1. Berkovic, G.; Krongauz, V.; Weiss, V. Chem Rev 2000, 100, 1741.
2. Kopelman, R. A.; Snyder, S. M.; Frank, N. L. J Am Chem Soc 2003, 125, 13684.
3. Gentili, P. L.; Ortica, F.; Favaro, G. Chem Phys Lett 2007, 444, 135.

4. Wojtyk, J. T. C.; Kazmaier, P. M.; Buncel, E. Chem Mater 2001, 13, 2547.
5. Dvornikov, A. S.; Rentzepis, P. M. Mol Cryst Liq Cryst 1994, 246, 379.
6. Zahavy, E.; Rubin, S.; Willner, I. J Chem Soc Chem Commun 1993, 23, 1753.
7. Zahavy, E.; Rubin, S.; Willner, I. Mol Cryst Liq Cryst 1994, 246, 195.
8. Weiss, V.; Friesem, A. A.; Krongauz, V. A.; Opt Lett 1993, 18, 1089.
9. Weiss, V.; Krongauz, V. A. J Phys Chem 1994, 98, 7562.
10. Fu, S.; Liu, Y.; Lu, Z.; Dong, L.; Hu, W.; Xie, M. Opt Commun 2004, 242, 115.
11. Krongauz, V. Isr J Chem 1979, 18, 304.
12. Hosotte, S.; Dumont, M. Synt Mate 1996, 81, 125.
13. Fu, S.; Hu, W.; Xie, M.; Wang, G.; Li, Y.; Duanmu, Q.; Tian, J.; Liu, Y. Phys B 2007, 400, 198.